Determination of the Plasmaparameters and the Suprathermal Microfields in a Critical Velocity Rotating Plasma

E. Möbius, A. Piel, and G. Himmel

Institut für Experimentalphysik II, Ruhr-Universität Bochum

Z. Naturforsch. **34 a**, 405–413 (1979); received January 24, 1979

In a critical velocity rotating plasma the profiles of the HeI 4471 Å and HeI 4922 Å lines have been investigated with high time resolution using an optical multichannel system in order to determine suprathermal electric microfields. The plasma density has been measured simultaneously with a CO_2 laserinterferometer. The existence of low- and highfrequency fields is proved by the occurrence of a strongly enhanced forbidden line component and plasma satellites in the front of the current spokes, which are typical for this plasma. Thus the occurrence of electrostatic instabilities and a turbulent heating process at the critical velocity is confirmed experimentally.

I. Introduction

The occurrence of a "critical velocity" in the interaction between a magnetized plasma and a neutral gas – the phenomenon at first was proposed by Alfvén in connection with his model on the origin of the Solar System [1] – has been reported by several authors [2, 3]. In a recent paper [4] by the authors of this article the existence of the relative motion between plasma and gas has been proved directly by Doppler shift measurements.

As has been pointed out in separate papers [5, 6], among all theoretical models [7] which try to explain the critical velocity phenomenon, only those turn out to be successful which involve turbulent heating of the electrons by means of a modified two-stream instability, similar to that proposed by Sherman [8] and Raadu [9]. It has been demonstrated by the authors that this process is located in the front of the observed current-spokes, which are found to be typical for such plasmas. Since this ionizing front is moving relative to the neutral gas at the critical velocity, the newly formed ions and electrons are separated by the magnetic field due to their different gyro radii. An azimuthal space charge electric field is created within the front leading to a secondary relative drift between electrons and ions. The drift velocity reaches the critical velocity, thus providing the initial conditions for electrostatic cross field instabilities, of which the modified two-stream instability is the most likely to occur. The ionization process is maintained by a strong turbulent electron heating caused by the instability [5].

In this article the existence of strongly excited electrostatic instabilities in the front of the spokes is proved more directly. For this reason the profiles of the HeI 4471 Å and HeI 4922 Å lines are carefully examined for the occurrence of suprathermal field fluctuations. – Those lines are already well known to be sensitive indicators for turbulent electric fields [10, 11].

This method, however, is limited to a parameter range of the rotating plasma in which the line intensities allow for both a good spectral and a high time resolution, i. e. the high current regime must be chosen. Therefore the knowledge of the plasma parameters has to be extended beyond that range which could be investigated by probes [6]. A CO_2 laserinterferometer is used instead, allowing for an exact separation of the nonthermal microfield from the line profiles.

II. Experimental and Data Handling

The rotating plasma is generated in a homopolar device, which is shown with the discharge circuit in Figure 1. The axial magnetic field is generated by

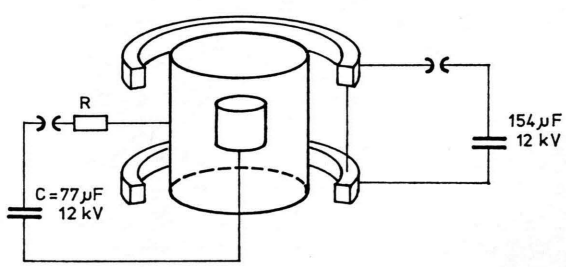

Fig. 1. Discharge circuit of the rotating plasma.

Reprint requests to Dr. E. Möbius, Institut für Extraterrestrische Physik, MPI für Physik und Astrophysik, D-8046 Garching bei München.

0340-4811 / 79 / 0400-0405 $ 01.00/0

two Helmholtz coils and attains a field strength up to 0.5 Tesla. The coils and the discharge current are each fed by a capacitor being switched by a spark gap. The discharge current is adjusted by a variable resistor. Extensive studies have been performed in the plasma over the current range up to $I_D \approx 1$ kA concerning the parameters and the spatial structure of the plasma [6]. But with respect to the need for high line intensities the diagnostic techniques have been extended to plasma densities higher than some 10^{20} m^{-3}, Langmuir probes then being inapplicable because of arcing. A CO_2 laserinterferometer yielding integral density information along the optical path is used instead. This technique provides an excellent extension of the results of our previous studies [6] into the high current regime.

1. Optical Registration and Arrangement

With respect to the purpose of this work – both good spectral and time resolution are needed – an optical multichannel analyzer (OMA) with high sensitivity is used for the optical registration. The exit slit of a 1 m grating monochromator is replaced by the detector head of the OMA, the image converter section of which can be operated as a fast shutter on a time scale of some hundred nanoseconds. The whole spectral information is stored in a 500 channel shift register. The overall intrument width is about 0.25 Å.

The whole optical arrangement including the CO_2 laserinterferometer can be taken from Figure 2. The plasmalight is recorded end-on focused to the entrance slit of the monochromator by 1 : 1 image, thus providing an optimum both in light intensity and spatial resolution. The evolution of the total plasmalight is recorded on the opposite side. The mirrors on either side of the plasma are supplied with a hole allowing for the measurement of density on the path of optical registration.

A Mach-Zehnder device is used as laserinterferometer. If the beams of its two branches coincide exactly between the second beam splitter and the detector, the variations of the central order of diffraction directly represent the evolution of the plasma density. – Pulsed laser operation is necessary to avoid thermal damage of the detectors.

Moreover a careful coordination in time of the whole experimental setup has to be fulfilled. The whole experiment is controlled by the internal cycle of the OMA. A special shutter control signals the right instant by means of a pulse. The timing of the signal pulse is measured either from the registering of a spoke passing by or from the moment of ignition. More detailed descriptions have been given elsewhere [12, 13].

2. Registration and Analysis of the Data

The optical as well as the interferometric registration yields only integral information along the optical path. Thus the axial variation of both the light intensity and the plasma density have been determined in addition by side-on studies of the He spectral lines.

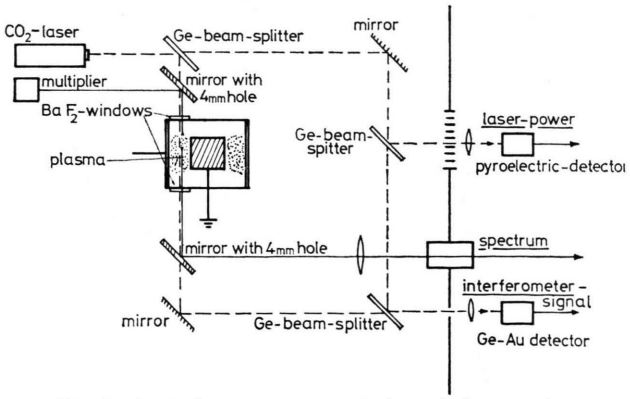

Fig. 2. Optical arrangement of the whole experiment together with the laser interferometer.

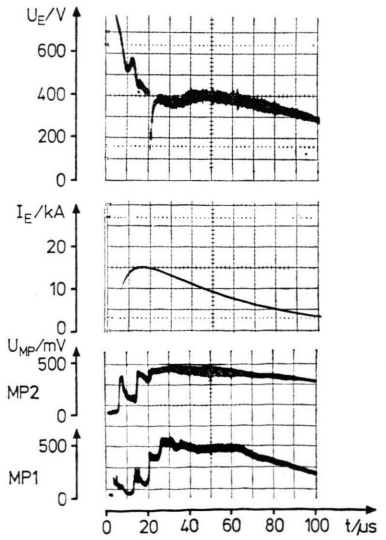

Fig. 3. Evolution of the high current discharge. From top to bottom: Discharge voltage, Discharge current, Total plasmalight recorded by two photomultipliertubes MP1 and MP2 at different azimuthal positions.

Together with the density shape the phase shift of the CO_2 laserinterferometer

$$\Delta\Phi = \frac{\pi}{\lambda\, n_c} \int_0^d n(z)\,\mathrm{d}z \qquad \text{(II, 1)}$$

gives the right absolute density $n\ (z)$, n_c meaning the cut-off density for the corresponding wavelength λ. The ambiguity of the phase in the interferometer amplitude

$$U_A = U_0 \sin(\Delta\Phi + \Phi_0) \qquad \text{(II, 2)}$$

is removed by taking the whole discharge. The maximum amplitude U_0 and the initial phase Φ_0 can also be found in this way. – The beam deflection expected in the most interesting steep density spokes is estimated to be negligable [13].

The digital data of the recorded line profiles will be interpreted by two different steps. – On one hand these data are smoothed over 2 to 5 channels each, if the counting rate is small. Thus even very small structures of the line profile amounting only 1% of the maximum intensity can be identified, though the spectral resolution is somewhat reduced.

On the other hand the corresponding profiles are calculated for the equivalent thermal plasma using the measured local density. The line profiles represent an average over the axial density shape as well as over parts of the steep density gradient of the spokes. They can be expressed as a linear superposition of profiles emitted from different regions,

$$I(\Delta\lambda) = \frac{\int_0^{n_{Max}} I(n, \Delta\lambda)\, V(n)\, L(n)\,\mathrm{d}n}{\int_0^{n_{Max}} V(n)\, L(n)\,\mathrm{d}n}, \qquad \text{(II, 3)}$$

where $V(n)$ and $L(n)$ respectively represent the fraction of plasma volume and the luminousity of the corresponding density n. $I(n, \Delta\lambda)$ represent theoretical profiles by Barnard et al. [14, 15], which have been confirmed experimentally to a good accuracy [16].

The light intensity is taken to be

$$L(n) \sim n \qquad \text{(II, 4)}$$

which is evident from earlier correlation measurements [6]. Moreover it has been proved that the spokes are aligned exactly parallel to the magnetic field with two acially displaced probes.

Doppler broadening and fine structure of the lines are already included in the above tables [14, 15]. Zeeman splitting is smaller than 0.1 Å producing only a small additional broadening, which is taken into account together with the instrument-width by a final convolution of the profile.

III. Analysis of the Plasma parameters in the High Current Discharge

Since the spectroscopic studies on the rotating plasma are restricted to the parameter range of very high currents, some information on the evolution of the discharge will be presented in this chapter, before the nonthermal fields are treated.

1. Temporal Evolution of the High Current Discharge

The temporal evolution of discharge voltage, discharge current and light intensity is compiled in Figure 3.

The whole discharge can be divided into three distinct phases. The build-up phase (1) is characterized by the well-known rotating spokes as can be easily seen on the light-signal. It must be emphasized that these are the same spokes, which have already been investigated in detail. Their motion is derived from the temporal displacement of both signals. In addition a high relative velocity between the plasma and the neutral gas has been proved by Doppler-shift measurements for the build-up phase [4, 12].

About 20 μs from ignition a plateau-phase (2) is found beginning with the maximum of the current. The discharge voltage as well as the light-intensity have reached a constant value, and the plasma has formed a nearly uniform disc with a high degree of ionization indicated by a strongly enhanced intensity of the HeII 4686 Å line [4, 12].

About 30 μs later the decay phase (3) begins, when the discharge voltage falls below the critical value. The discharge current has then decreased significantly.

The temporal evolution of the plasma density, evaluated from the interferometer phase, also reproduces these three phases as can be seen from Figure 4. The reported mean density has been obtained under the assumption that the plasma fills the whole electrode chamber, which is found to be true for the ignition and the decay phase. It is emphasized that the characteristic shape of the spokes with its steep increase of the density and the smooth decrease in the rear is proved for the high current regime as well as for the remaining parameter range. By direct comparison of the light-signal and the floating poten-

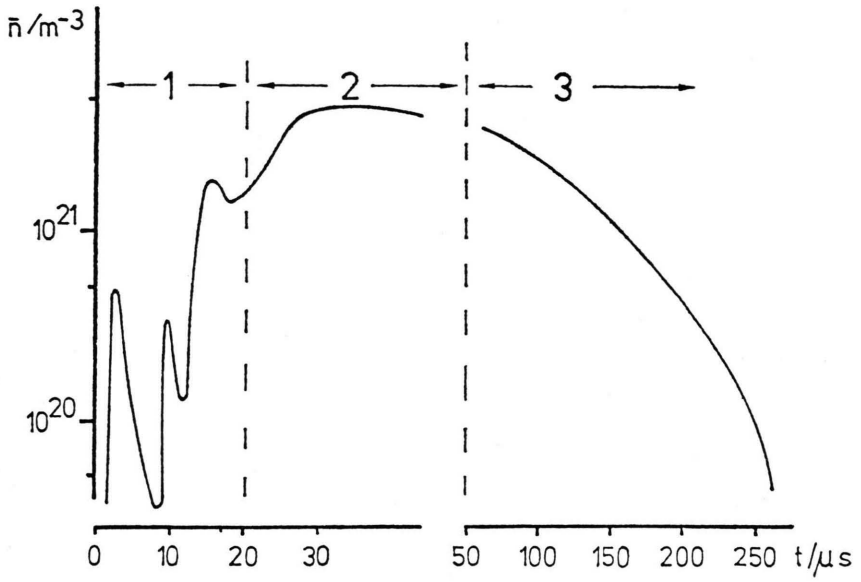

Fig. 4. Evolution of the mean plasma density in the high current discharge.

tial, the same potential structure as is usually connected with those spokes [5] has been verified. The subsequent plateau phase is discussed elsewhere [13] in more detail.

Since a diffusion shape for the density occurs during the afterglow, the decay phase will be suitable for a direct comparison of the interferometric and the spectroscopic results with respect to their consistency. The investigation of turbulent microfields, however, is confined to the build-up phase, when a particularly strong turbulent electron heating connected with detectable electric fields is expected in the front of the spokes, thus providing an extremely high ionization rate.

In addition the build-up phase has been studied with respect to impurity lines in the interesting spectral range. Because of the occurrence of OII lines near the HeI 4471 Å line the HeI 4922 Å line is more suitable for the investigation of turbulent features except very close to the ignition [13].

2. *Comparison of Interferometric and Spectroscopic Density Values*

For a direct comparison of the different methods the line-profile as well as the interferometer signal are recorded simultaneously along the same path through the plasma. In Fig. 5 a all the monitoring traces are compiled. On the first diagram the exposure time (opening pulse) can be compared to the interferometer phase ($\Delta\Phi(U_{D1})$). The second diagram shows the interferometer amplitude and its initial phase as well as the laser-power (pyroelectric detector). Moreover the discharge current is given.

The profile of the HeI 4471 Å line has been calculated as described in the last chapter. In Fig. 5 b it is compared to the spectrum recorded by the OMA. A very good agreement is found. These investigations have been performed at various instants during the decay phase for different gas pressures. The plasma densities obtained by both

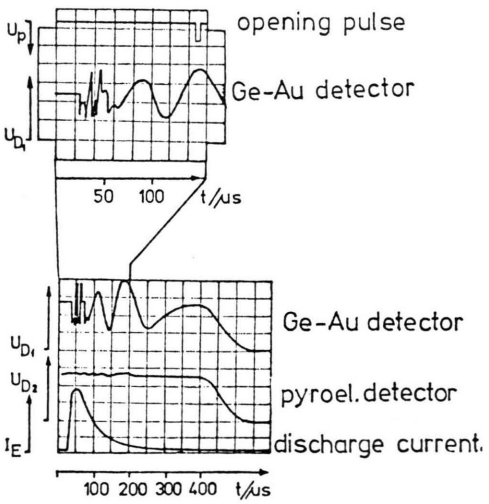

Fig. 5 a. Measurement of plasma density by interferometer — oscilloscopic curves —.

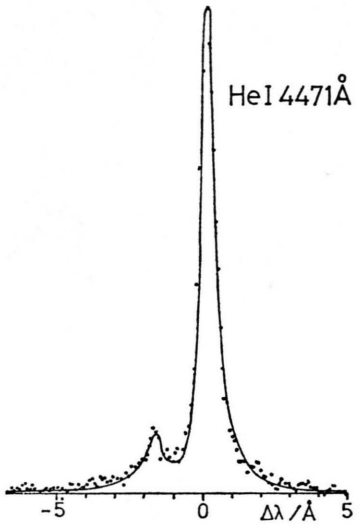

Fig. 5 b. Comparison of the measured and the calculated line profile during the decay phase. ——— calculated profile, $\bar{n} = 1.6 \cdot 10^{20}\,\mathrm{m}^{-3}$, ···· O.M.A. spectrum, $\Delta t = 150\,\mu\mathrm{s}$.

methods are compiled in Figure 6. Taking into account all sources of error, the interferometer phase, the density shape and the light distribution, an error bar of 20% turns out to be realistic. In the limits of experimental precision both methods are proved to be in agreement. From side-on studies of the total plasma light and helium line profiles the first spokes of the discharge have been proved to spread along the whole discharge chamber in the axial direction [13]. Thus the laser interferometer is a powerful instrument even in the interesting build-up phase.

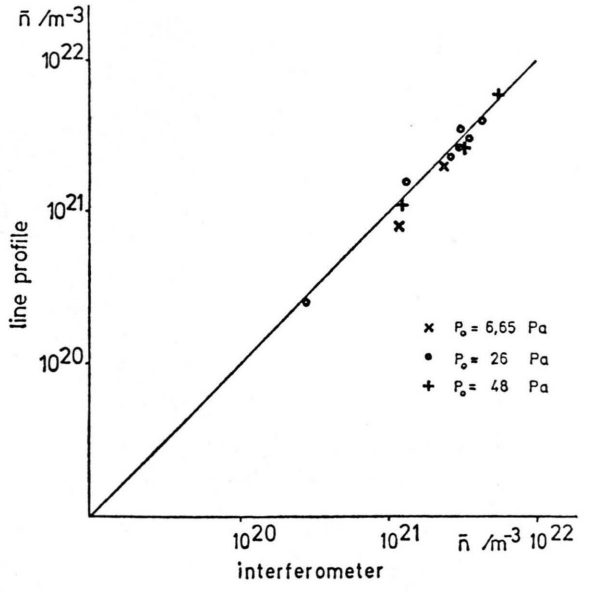

Fig. 6. Comparison of the density values obtained by both methods (interferometer and line profile).

IV. Investigation of the Suprathermal Electric Fields

In view of the results of the previous chapter regarding the plasma parameters of the discharge and the applicability of the interferometer as an independent diagnostic tool, those features of the line profiles, which are due to turbulent fields, can now be separated.

1. Evolution of a HeI Line-Profile over the First Spoke

In Fig. 7 the profile of the HeI 4471 Å line is presented, which is recorded when the first spoke of the discharge just arrives at the optical path. The exposure time is marked by the opening pulse for the vidicon. On either side of the forbidden component, plasma satellites can be detected, the distance of each being $\Delta\lambda = 0.4$ Å. From this value a plasma density of $n \approx 5 \cdot 10^{19}\,\mathrm{m}^{-3}$ is obtained, which is too

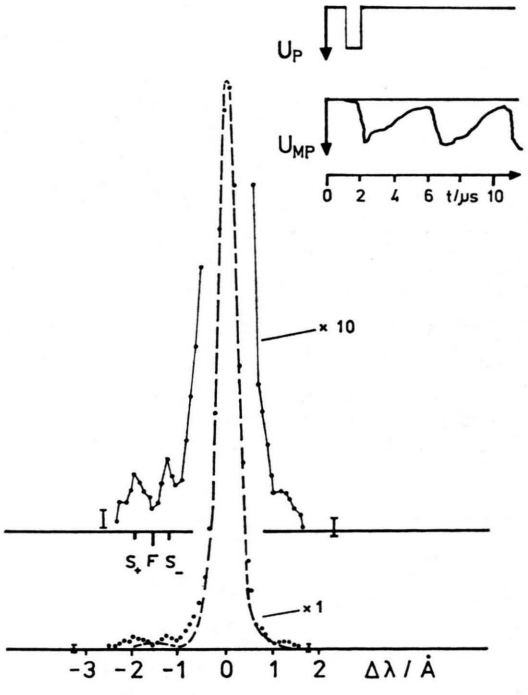

Fig. 7. Profile of the HeI 4471 Å line, when the first spoke arrives. ——— profile with $\bar{n} = 5 \cdot 10^{19}\,\mathrm{m}^{-3}$. On top right: opening pulse for the vidicon $U_P(t)$, plasma light $U_{MP}(t)$.

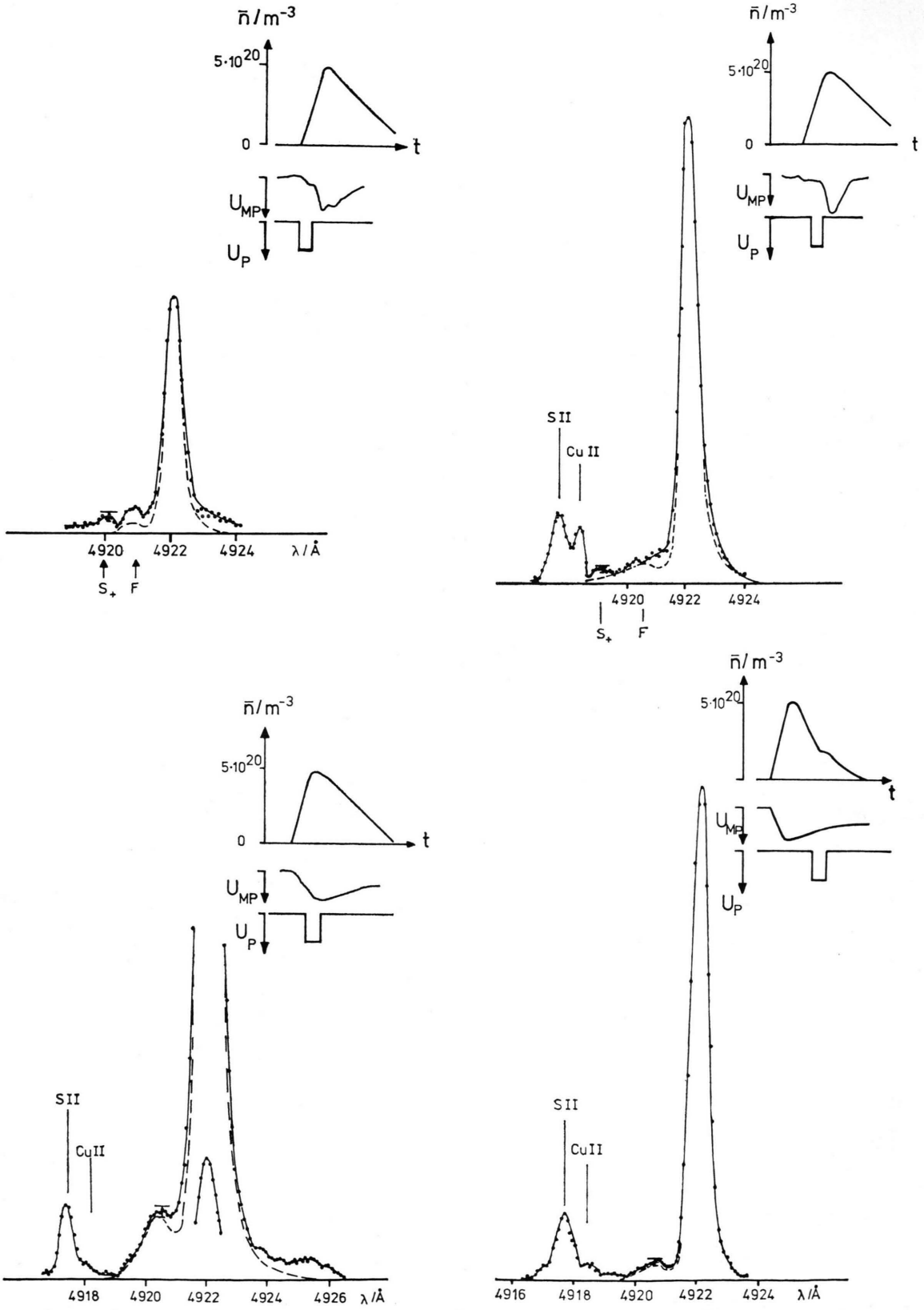

Fig. 8 a, b, c, d. Evolution of the profile of the HeI 4922 Å-line over the first spoke; in each picture there are shown: evolution of the density $n(t)$, plasma light $U_{MP}(t)$, opening pulse for the vidicon $U_P(t)$.

small, however, to be measured by the interferometer. It is not advantageous to use the HeI 4471 Å line following the spoke up to higher densities because of the troubles with the OII lines mentioned above.

Therefore the remaining investigations are performed using the corresponding singlet line HeI 4922 Å. Its evolution over the first spoke is presented in Fig. 8 together with plasma density, light intensity and the opening pulse. The variation of the integrated line intensity corresponds to the light signal.

The statistics of the counting rate have been improved by smoothing over 5 channels and the resulting error bar is marked in each profile. – Besides the helium line several impurity lines arise, which have been identified in previous investigations [13]. The theoretical line profiles are drawn in dashed lines. They are normalized to the same maximum intensity in order to emphasize the surplus area of the turbulent line structures.

On the line profiles emitted from the front of the spoke, considerable deviations from the thermal profile are indeed found. In the first picture (Fig. 8 a) the far satellite S_+ can be detected, and the forbidden component yields twice the theoretical value for the intensity. As the density rises (Fig. 8 b) the distance of the far satellite increases, as to be expected for a structure, which is connected with the plasma frequency. From the measured separation of the satellites

a) $\Delta\lambda = 1$ Å and b) $\Delta\lambda = 1.5$ Å

the plasma density yields

a) $n = 2.1 \cdot 10^{20}\,\mathrm{m}^{-3}$ and b) $n = 4.6 \cdot 10^{20}\,\mathrm{m}^{-3}$

which are in good agreement with interferometric values. At these densities the near satellite S_- merges with the allowed line and thus cannot be found separately.

A further deviation of the line profile (see Fig. 8 b) is the smoothing of the valley between both components of the line, which is even much stronger than observed normally. This smoothing has been found on the HeI 4471 Å line, too.

When the maximum density of the spoke has been reached, however, (Fig. 8 c), the far satellite vanishes, and the two components are separated again. From the rear zone of the spoke (Fig. 8 d) an exactly thermal line profile is emitted indicating a quiet plasma with no turbulent effects.

2. *Evaluation of the Nonthermal Microfields from the Line Profiles*

The interpretation of these profiles is based on the assumption of no correlation between thermal and nonthermal microfields. Thus the mean squares of the single field strengths can be added forming the total field which acts on the atoms.

$$\langle E_{\mathrm{tot}}^2 \rangle = \langle E_{\mathrm{therm}}^2 \rangle + \langle E_{\mathrm{turb}}^2 \rangle \,. \qquad \text{(IV, 1)}$$

From the enhanced forbidden component, marked with F in the figures 7 and 8, the low frequency turbulent field can be extracted. According to Baranger and Mozer [10] the field strength is calculated from the ratio S of the surplus area of the forbidden component to the area of the allowed line.

$$\langle E_{\mathrm{turb}}^2 \rangle \frac{V^2}{m^2} = 4.5 \cdot 10^8 \, S \,. \qquad \text{(IV, 2)}$$

The values have been specified to the HeI 4922 Å line. From this relation the low frequency field is $E = 4.8 \cdot 10^5$ V/m. The value can be compared with a probable saturation value of the modified two-stream instability due to ion trapping [16]. This means that the total kinetic energy of the ions is transformed into field fluctuations, which yields

$$E_{\mathrm{tr}} \approx \frac{W_{\mathrm{i}}}{e} \cdot k \approx \frac{W_{\mathrm{i}}}{e} \cdot \frac{\omega_{\mathrm{LH}}}{V_{\mathrm{cr}}} \,. \qquad \text{(IV, 3)}$$

k being the wavenumber and ω_{LH} the lower hybrid frequency. Under the experimental conditions, a field strength $E_{\mathrm{tr}} \approx 7 \cdot 10^5$ V/m is found which agrees well with the experimental result.

Regarding the plasma satellites observed in the front of the spoke the occurrence of high frequency field is evident, too. Obviously those oscillations at the plasma frequency are excited due to some secondary processes during the nonlinear development of the primary low frequency instability. Following the further evolution of the spoke the band of excited frequencies spreads, and is especially observed between the forbidden and the allowed line. The main part of the near satellite, however, merges with the allowed line. Therefore the quantitative treatment cannot be done according to the simple approach of Baranger and Mozer [10]. A more realistic treatment of the dynamic Stark effect for the total range of frequencies has been reported by Autler and Townes [17]. A short discussion of the main results and the application to the problem above have been presented in another paper [13].

It must be emphasized that the near satellite really changes its identity with the allowed line, if its distance from the forbidden component equals the splitting of both components. Nevertheless the mean field strength of the high frequency fields can be obtained from the far satellite. As can be derived from the more sophisticated treatment of Autler and Townes the approximation of Baranger and Mozer holds for the far satellite even in the resonance case. Thus the relation

$$\langle E_{\mathrm{turb}}{}^2 \rangle = 2.1 \cdot 10^7 \, S_+ \, [(\omega_{\mathrm{ab}} - \omega_{\mathrm{pe}})/\mathrm{cm}^{-1}] \quad \text{(IV, 4)}$$

is used ω_{ab} being the level splitting and ω_{pe} the plasma frequency. A field strength of about $E \approx 7 \cdot 10^5$ V/m is calculated from the satellites in Fig. 8 a and 8 b.

3. Discussion of the Results

Low frequency microfields of $E = 4.8$ kV/cm have been proved to arise in the front of the first spoke of the rotating plasma under consideration. The evaluated field strength agrees with the values expected from a modified two-stream instability saturated due to ion trapping. These experimental results give direct evidence for a model of the critical velocity which involves the onset of the modified two-stream instability in the ionizing front thus providing the rapid ionization process by turbulent heating [5].

In addition field fluctuations at the electron plasma frequency have been observed spreading over a broader spectrum later on. Thus some secondary processes occur during the nonlinear phase of the two-stream instability, which allow the energy to be converted directly into electron plasma oscillations.

The evolution of the helium line profiles over the spoke is found to be in good agreement with earlier results on the azimuthal structure of the plasma [5, 6] and the given model of the critical velocity. In particular separation of the spoke into two distinct regions is observed again. Suprathermal microfields have been detected in the front of the spoke, thus proving the occurrence of electrostatic instabilities, where in fact the turbulent heating is expected in connection with the observed rapid ionization. On the contrary a thermal line profile is emitted from the rear part of the spoke, thus confirming the ohmic heat balance of the electrons, which has already been suggested by the probe measurements [6].

Moreover it is well understood that the turbulent fields could be detected only during the build-up phase of the high current discharge, since the relative motion between plasma and gas, which is known to be essential for the interaction at the critical velocity, is restricted to that phase [4].

The further development of the rotating plasma in the high current regime leads to densities exceeding $n = 5 \cdot 10^{20}\,\mathrm{m}^{-3}$ by far. Therefore it is then impossible to find any turbulent structures on the line profiles, since thermal microfields would have exceeded their nonthermal counterparts to the same degree. At the same time the conductivity of the plasma due to Coulomb collisions (see Spitzer [18]) will be sufficient for the actual discharge current as soon as the density exceeds $n = 6 \cdot 10^{20}\,\mathrm{m}^{-3}$. That means, a quenching of the instability in the front of the spoke has to be expected as well as a better electron heating all over the spoke. In the end the spoke must be smeared out due to plasma production in the rear. The typical character of the spoke is lost and finally a uniform disc is formed with a very high degree of ionization.

V. Conclusions

In this work the knowledge of the structure and the plasma parameters has been extended to the range of high discharge currents, of more than 10 kA, for the critical velocity rotating plasma. With the aid of this background information the profiles of the HeI 4471 Å and the HeI 4922 Å lines were evaluated with a time resolution better than 1 μs allowing for results concerning the temporal evolution of the current spokes, which survive in the build-up phase of the high current discharge. The plasma density was measured simultaneously by means of a CO_2 laserinterferometer.

In the front of the first spoke satellite structures at the plasma frequency as well as an intensified forbidden component on the profiles of the helium lines were proved. From these results direct evidence is given for both high-frequency and low-frequency turbulent microfields, the strengths of which have been found to agree with the estimated values for saturation of the modified two-stream instability due to ion trapping. In the rear part of the spoke, however, no suprathermal electric fields could be detected. Thus a direct confirmation is gained for the picture drawn on the current spokes from the

earlier investigations by Langmuir probes. The electrostatic instabilities responsible for the turbulent heating and the rapid ionization are indeed observed in front of the spoke, and a thermal plasma behaviour is found in the rear, where the classical heat balance holds.

Our present and earlier [6] results concerning the critical velocity phenomenon may now be summarized. We conclude that our model of the critical velocity, which is based on turbulent electron heating in an ionizing front [5], is confirmed by three crucial experimental observations:

- turbulent heating is necessary for the particle balance
- the starting conditions for the modified two-stream instability are realized in the front of the spokes
- suprathermal microfields have been detected in the front of the spokes.

Finally, returning from the laboratory to Alfvén's cosmogonical model, the *collective plasma process at the critical velocity*, as it was first proposed by Alfvén [1], must be accepted now as a reality. In all further investigations, however, a distinct structure of the interaction region, similar to an ionizing front, has to be taken into account. But the real importance for the early solar nebula can only be proved by detailed theoretical calculations with parameters scaled to cosmical dimensions.

Acknowledgements

We are grateful to Prof. Dr. H. Schlüter for valuable discussion and encouragement. The investigations are part of the joint efforts within the Sonderforschungsbereich 162 "Plasmaphysik Bochum/Jülich".

[1] H. Alfvén, On the Origin of the Solar System, Oxford University Press, Oxford 1954.
[2] U. V. Fahleson, Phys. Fluids **4**, 123 (1961).
[3] B. Angerth, L. Block, U. Fahleson, and K. Soop, Nucl. Fus. Suppl. Part **I**, 39 (1962).
[4] G. Himmel, E. Möbius, and A. Piel, Z. Naturforsch. **32 a**, 577 (1977).
[5] A. Piel, E. Möbius, and G. Himmel, Sonderforschungsbereich Plasmaphysik Bochum/Jülich, Report No. 78-M2-037 (1978).
[6] G. Himmel, E. Möbius, and A. Piel, Z. Naturforsch. **31 a**, 934 (1976).
[7] J. C. Sherman, Astrophys. Space Sci. **24**, 487 (1973).
[8] J. C. Sherman, Nobel Symposium No. **21** (1972).
[9] M. A. Raadu, Division of Electron and Plasma Physics, Royal Inst. of Technology Stockholm Report No. TRITA-EPP-75-28 (1975).
[10] M. Baranger and B. Mozer, Phys. Rev. **123**, 25 (1961).
[11] H. J. Kunze, H. R. Griem, A. W. De Silva, and G. C. Goldenbaum, Phys. Fluids. **12**, 2669 (1969).
[12] G. Himmel, E. Möbius, and A. Piel, Sonderforschungsbereich Plasmaphysik Bochum/Jülich, Report No. 77-M2-024 (1977).
[13] E. Möbius, A. Piel, and G. Himmel, Sonderforschungsbereich Plasmaphysik Bochum/Jülich, Report No. 78-M2-036 (1978).
[14] A. J. Barnard, J. Cooper, and E. W. Smith, J. Quant. Spectros. Radiat. Transfer. **14**, 1025 (1974).
[15] A. J. Barnard, J. Cooper, and E. W. Smith, J. Quant. Spectros. Radiat. Transfer. **15**, 429 (1975).
[16] D. Biskamp, Nucl. Fus. **13**, 719 (1973).
[17] S. H. Autler and C. H. Townes, Phys. Rev. **100**, 703 (1955).
[18] L. Spitzer, Physics of Fully Ionized Gases, John Wiley & Sons, New York 1967, p. 133.